

Effects of Bias Voltage on Diamond Like Carbon Coatings Deposited Using Titanium Isopropoxide (TIPOT) and Acetylene/Argon Mixtures onto Various Substrate Materials

R. Said¹, C. A. A. Ghumman², O. M. N. D. Teodoro²,
W. Ahmed^{1,*}, A. Abuazza³, and J. Gracio⁴

¹School of Computing, Engineering and Physical Sciences, University of Central Lancashire, Preston PR1 2HE, UK

²CEFITEC, Department of Physics, Faculty of Science and Technology, New University of Lisbon, 2829-516 Caparica, Portugal

³Department of Physics, Faculty of Science, University of Alfateh, Tripoli, Libya

⁴Centro de Tecnologia Mecânica e de Automação, Universidade de Aveiro, 3810-193 Aveiro, Portugal

RF-PECVD was used to prepare amorphous of carbon (DLC) onto stainless steel 316 and glass substrates. The substrates were negatively biased at between 100 V to 400 V. Thin films of DLC have been deposited using C₂H₂ and titanium isopropoxide (TIPOT). Argon was used to generate the plasma in the PECVD system chamber. DEKTAK 8 surface stylus profilometer was used to measure the film thickness and the deposition rate was calculated. Micro Raman spectroscopy was employed to determine the chemical structure and bonding present in the films. Composition analysis of the samples was carried out using VGTOF SIMS (IX23LS) instrument. In addition, X-ray photoelectron spectroscopy (XPS) was used to analyze the composition and chemical state of the films. The wettability of the films was examined using the optical contact angle meter (CAM200) system. Two types of liquids with different polarities were used to study changes in the surface energy. The as-grown films were in the thickness range of 200–400 nm. Raman spectroscopy results showed that the I_D/I_G ratio decreased when the bias voltage on the stainless steel substrates was increased. This indicates an increase in the graphitic nature of the film deposited. In contrast, on the glass substrates the I_D/I_G ratio increased when the bias voltage was increased indicates a greater degree of diamond like character. Chemical composition determined using XPS showed the presence of carbon and oxygen in both samples on glass and stainless steel substrates. Both coatings the contact angle of the films decreased except for 400 V which showed a slight increase. The oxygen is thought to play an important role on the polar component of a-C.

Keywords: Diamond Like Carbon (DLC), Chemical Vapour Deposition (CVD), Raman Spectroscopy, Contact Angle, SIMS.

1. INTRODUCTION

There has been considerable interest in diamond-like carbon (DLC) films due to their highly desirable properties such as high hardness, low friction, high wear resistance and chemical inertness. These make the DLC films highly suitable for use in various applications, such as in cutting tools, biomedical implants and optical components. In recent years, for example, amorphous DLC films have been widely utilized as hard coatings with useful optical, thermal and electrical properties.^{1,2} In addition,

DLC films have a wide band gap and their refractive indices can be readily adjusted during the film deposition process. The films have been utilized as protective coatings for IR windows and anti-reflective coatings for solar cells.³⁻⁵ The structure of DLC films in particular plays a key role in determining their properties, which result from the combination of the sp² bonding as in graphite and sp³ bonds found in the diamond structure. A number of processes including RF cathodic deposition, RF/DC sputtering, unbalanced magnetron sputtering, arc evaporation and plasma CVD have been used to deposit DLC films and Me-DLC.⁶⁻¹² The type of deposition technique employed has strong influence on the properties of the deposited

*Author to whom correspondence should be addressed.

coating and on the scaling to large scale production. The process parameters, which can be varied over a wide range, can be used to deposit carbon-based coatings with different properties. For industrial applications, the reactor design and the process parameters need to be optimised in order to deposit films with the most desirable characteristics. In comparison, with other deposition processes CVD gives better control, reproducibility, higher throughput and has the ability to coat complex geometry substrates due to its high throwing power.

For many applications including microelectromechanical systems (MEMS) application, the surface energy of the films is very important. The wettability properties of the ta-C films can be adjusted by incorporating different metals into the DLC films.^{13–15} Regardless of the deposition technique employed the synthesis of DLC films showed that applying a negative bias voltage to the substrate had a profound influence on the film properties.¹⁶

This investigation is aimed at evaluating the potential of a more readily available synthetic titanium modified DLC film for possible biomedical applications. In this paper, four types of DLC films were deposited onto stainless steel substrates and glass using plasma CVD. DLC films were deposited on different substrates at varying bias voltages. The as-deposited DLC films were characterized using a number of techniques including Raman spectroscopy, SIMS, XPS, CAM 200 analyses and the results obtained are reported.

2. EXPERIMENTAL DETAILS

The CVD system used consisted of a capacitively coupled asymmetric plasma reactor driven by a 13.56 MHz RF power supply, connected to the upper electrode. The source gases were uniformly distributed by a showerhead type distributor, placed in contact with the superior electrode. Stainless steel 316 and glass were used as the substrates material and various bias voltages, which was placed on the lower electrode. Acetylene (C₂H₂) and titanium isopropoxide [TIPOT]—Ti [OCH₂CH₃]₄, were used as precursors for DLC deposition. The substrates prior to deposition were cleaned using plasma etching using acetone and argon ions in an RF discharge (for 2 minutes). Table I shows the deposition conditions employed to prepare the DLC samples. The DLC coatings into stainless steel and glass were deposited with different negative bias voltage ranging from 100–400 V. Film thickness was measured using DEKTAK 8 surface stylus profilometry. X-ray photoelectron spectroscopy (XPS) was used to characterize the presence/absence of titanium in the DLC samples. SIMS technique with depth profiling was used to characterize the titanium in the coatings using VGToF SIMS (IX23LS). Raman spectrometer was employed to investigate the chemical structure of amorphous carbon matrix. Optical contact angle meter (CAM200) was used

Table I. PECVD conditions employed for DLC deposition.

Parameter	Value
Deposition gases	TIPOT, Ar, C ₂ H ₂
TIPOT flow rates (sccm)	10
C ₂ H ₂ flow rate (sccm)	10
Ar flow rate (sccm)	10
Base pressure (Torr)	3.6–6.4 × 10 ⁻⁶
Working pressure (<i>P_w</i>)-Torr	1.7–4 × 10 ⁻²
RF power (W)	82–116
Substrates	Stainless steel-glass
Substrate temperature (°C)	25
Bias voltage (V)	100–200–300–400

to measure the contact angle. Surface energy of the films was determined using the contact angle measurements. The Young's equation correlates the surface energy with contact angle of liquid and solid surface.¹⁷

$$\gamma_{sv} = \gamma_{sl} + \gamma_{lv} \cos \theta \quad (1)$$

Where γ_{sv} and γ_{lv} are the solid and liquid surface energy respectively; γ_{sl} is the solid/liquid interfacial energy and θ contact angle. In order to determine the surface energy of the solid, contact angle measurements were employed. The harmonic-mean method¹⁸ was used in this study

$$(1 + \cos \theta) \gamma_{lv} = 4 \left\{ \frac{\gamma_{sv}^d \gamma_{lv}^d}{\gamma_{sv}^d + \gamma_{lv}^d} + \frac{\gamma_{sv}^p \gamma_{lv}^p}{\gamma_{sv}^p + \gamma_{lv}^p} \right\} \quad (2)$$

In the case of two liquids, the values of γ_{lv}^d and γ_{lv}^p for these liquids are known, the depressive and polar components of the solid surface energy can be obtained by solving the two simultaneous equations.

3. RESULTS AND DISCUSSION

Figure 1 shows the deposition rate of the films coatings on the stainless steel substrates. The deposition rate was increased when increasing negative bias voltage. These results were qualitatively similar with other research.¹⁹ When the negative bias voltage was applied the plasma intensity near the substrate was also increased due to a greater degree of ionisation which generates a higher concentration of positive ions. These are accelerated towards the substrate causing enhanced growth. At much high bias voltages in excess of –300 V the deposition rate levels off, this may be due to the sputtering effect which cancels out the enhanced plasma intensity.

The Raman spectra acquired between 1000 and 2100 cm⁻¹ from DLC films deposited onto the stainless steel and glass substrates is shown in Figure 2. All the spectra reveal a typical DLC structure characterized by one band composed of the main G (graphite) peak and D (disordered) shoulder. This is in contrast to graphite that typically two separate peaks dependent on the bias voltage. The G and D band positions are shown in Table II. The

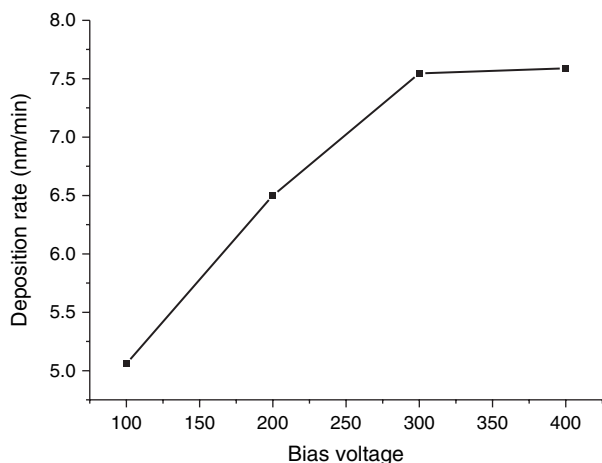


Fig. 1. Deposition rate of the films on the stainless steel substrates.

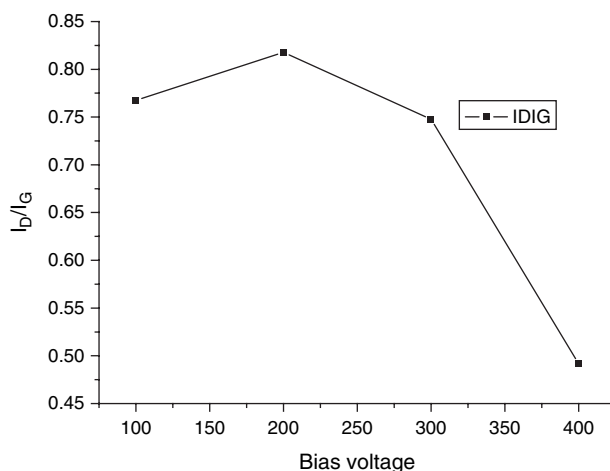


Fig. 3. I_D/I_G ratio of the films onto stainless steel substrates versus bias voltage.

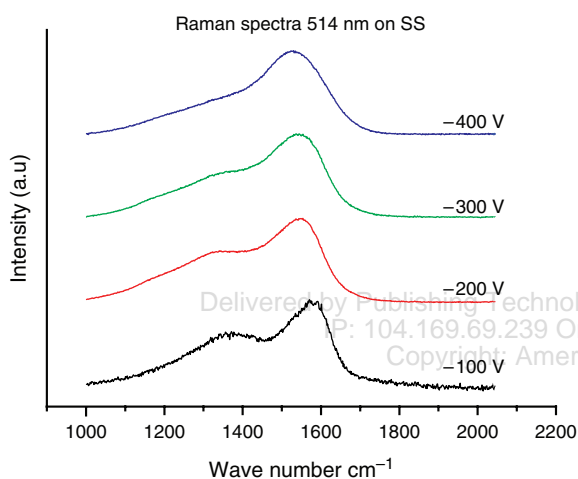


Fig. 2. Raman spectra of DLC films onto stainless steel substrates with various bias voltages.

coatings on stainless steel show the G-peak position shifted to lower frequencies with decreasing of I_D/I_G which indicates an increase in the fraction of sp^3 bonds. The I_D/I_G ratios were calculated at various values of the substrates voltage and these results have been plotted in Figure 3. In general, the I_D/I_G ratio decreases indicating a reduction in the sp^3 characteristics of the films even though the graphs show a slight increase at -200 V. This is within the statistical variance. However, the coatings on glass reveal

Table II. Experimental results from Raman spectroscopy with various substrates and bias voltage.

Bias voltage	Glass			Stainless steel		
	G band	D band	I_D/I_G	G band	D band	I_D/I_G
100	1550.957	1431.684	0.194	1578.069	1388.9144	0.7677
200	1536.354	1363.376	0.426	1550.511	1370.6740	0.8177
300	1538.553	1370.003	0.473	1549.939	1379.7479	0.7478
400	1540.043	1364.374	0.592	1540.434	1356.7905	0.4917

that the G-peak position shifted to higher frequencies with increasing of I_D/I_G which means a increase in the fraction of sp^3 bond as shown in Figures 4, 5.

Figure 6 shows the contact angle with water, as function of the bias voltage for stainless steel and glass substrates. For both films coatings the contact angle decreased as increasing bias voltage up to -300 V with a slight increase at -400 V. This is may be due to the incorporation the oxygen into the films, with the surface energy ranging from 38–41 (mN/m). It is well known that the surface energy results reveal important thermodynamic properties of the films. Generally, the higher the surface energy of the solid substrate relative to the surface tension of the liquids, the better is the hydrophilicity. The smaller the contact angle the better the adhesion of water to the surface. Surface energy arises from the imbalance of the force between atoms or molecules at the interface. Several

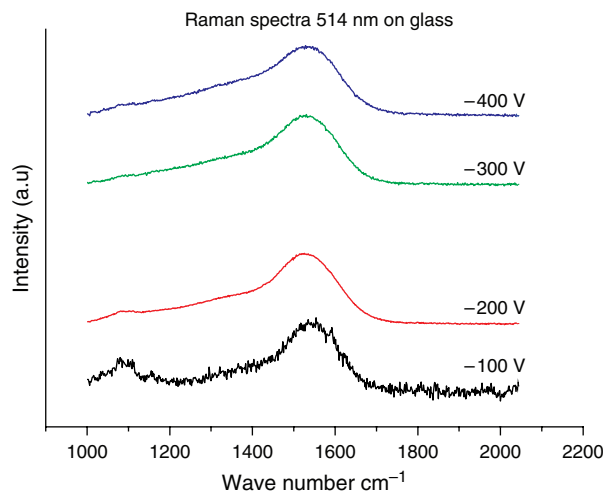


Fig. 4. Raman spectra of DLC films onto glass substrates with various bias voltages.

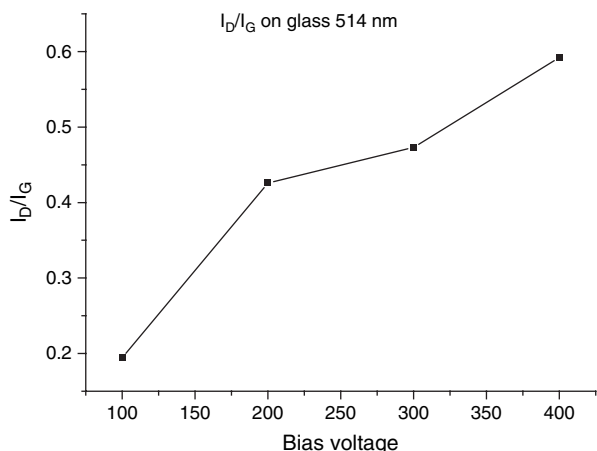


Fig. 5. I_D/I_G ratio of the films onto glass substrates versus bias voltage.

types of van der Waals interactions contribute to the surface energy that is dictated by two factors, dispersive γ_{iv}^d and polar γ_{iv}^p .²⁰ The dispersive contribution is derived from a single interaction generated by the movement of electrons around an atom or molecule. This depends on the type of material and its density. Figures 7, 8 show the surface energy as function of bias voltages onto stainless steel and glass respectively. The surface energy, dispersive and polar component was calculated by using the contact angle for two liquids according to the Eq. (2) as shown in Tables IV, V. The Table III shows the parameters used to Eq. (2). The polar component is built up from different forces/interactions, like hydrogen bonds, covalent bonds and dipole–dipole interactions. This increased the polar contribution of the surface bonding states obtained due to oxygen incorporation.

Figure 9 shows the surface composition of the DLC films on glass and stainless steel derived from the C1s and O1s photoelectron core level XPS. Surprisingly, no titanium is detectable. This may be due to the sensitivity of

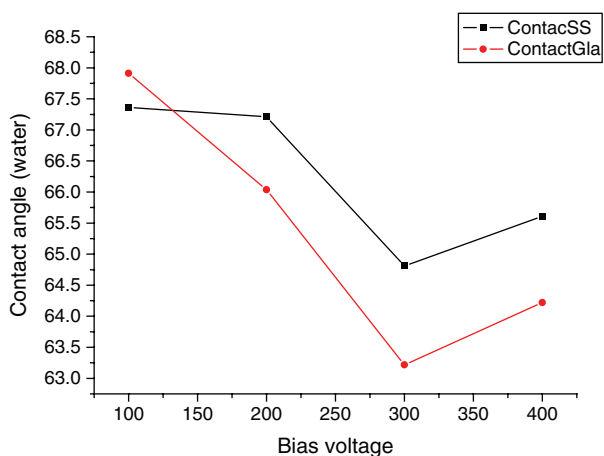


Fig. 6. Contact angle of water on the stainless steel and glass versus bias voltage.

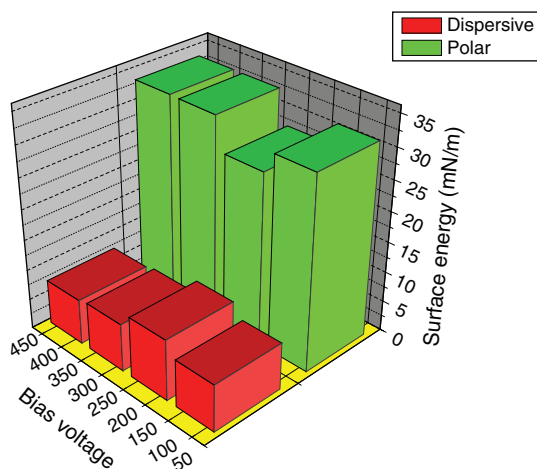


Fig. 7. Surface energy versus bias voltage onto stainless steel substrates.

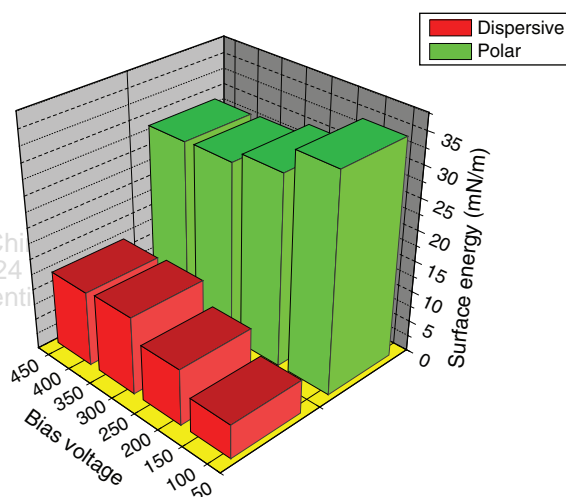


Fig. 8. Surface energy versus bias voltage onto glass substrates.

XPS instrument used. SIMS analysis has shown the presence of Ti in the films.

The positive ion ToF-SIMS spectra of a typical DLC surface layer (deposited at 20 sccm flow rate) is shown in Figure 10. Liquid metal ion source (Ga^+) was used at bombardment energy of 12 kV. Key ions such as H^+ , C^+ , $C_2H_3^+$, Ga^+ can be seen on the spectrum. The surface did not show any trace of the Ti metal in the film. Etching procedures were employed in order to dig into the film to see if Ti could be detected. Titanium could either be

Table III. The dispersive γ_{iv}^d and polar γ_{iv}^p components and total surface tension γ_{iv} for selected test liquid.

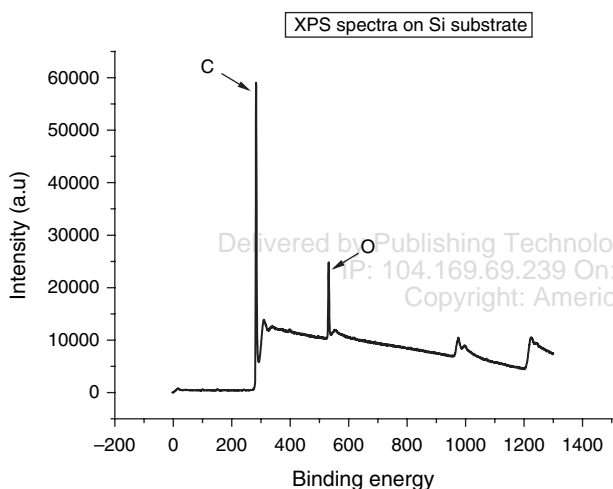
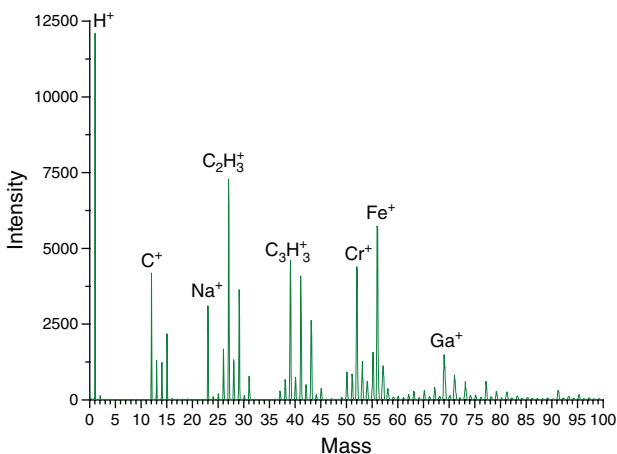
Liquid	γ_{iv}^d (mN/m)	γ_{iv}^p (mN/m)	γ_{iv} (mN/m)
Water	22.1	50.7	72.8
Ethylene glycol	29.29	18.91	48.2

Table IV. The dispersive γ_{sv}^d and polar γ_{sv}^p components and total surface energy γ of different bias voltage onto stainless steel substrate.

Bias voltage (V)	γ_{sv}^d (mN/m)	γ_{sv}^p (mN/m)	γ (mN/m)
100	7.790	31.543	39.333
200	9.731	29.112	38.843
300	7.866	33.428	41.294
400	7.415	33.478	40.893

Table V. The dispersive γ_{sv}^d and polar γ_{sv}^p components and total surface energy γ of different bias voltage onto glass substrate.

Bias voltage (V)	γ_{sv}^d (mN/m)	γ_{sv}^p (mN/m)	γ (mN/m)
100	5.503	34.808	40.311
200	9.090	30.776	39.866
300	12.540	28.883	41.423
400	12.085	28.642	40.727

**Fig. 9.** XPS Spectra of DLC with bias voltage (300 V) onto silicon substrates.**Fig. 10.** Positive ion ToF-SIMS spectra of DLC surface layer. Liquid Metal Ion source (Ga^+) was used at bombardment energy of 12 KV.

playing the role of a catalyst in influencing the properties of the DLC films without being actually incorporated into the depositing films. It is plausible that titanium may be present in our samples but we are unable to detect it using the techniques we have employed in this study (SIMS, XPS). However, in another study the SIMS technique has been used successfully to detect chromium (Cr) in their DLC films deposited using magnetron sputtering technique.²¹ Therefore, it should be possible to detect titanium using the same SIMS technique in our case and therefore requires further investigation.

4. CONCLUSIONS

RF-PECVD system was used to deposit DLC films onto stainless steel 316 and glass substrates under different bias voltage. The growth rate of DLC films increased with increasing bias voltages. Raman spectroscopy results displayed the typical D and G bands characteristic of DLC. The I_D/I_G ratio increased for the films deposited on glass substrates indicating a higher fraction of sp^3 bonding in the samples. However, the DLC coatings onto stainless steel substrates I_D/I_G increased at lower bias voltages but decreased for higher bias voltages. The contact angle values decreased with increasing bias voltage and then increased slightly beyond 300 V. Surface energy values were calculated for glass and stainless steel from the contact angle measurements. There was no significant overall difference in the surface energy between the substrates at the bias voltages investigated. However, clearly there were differences in the polar and dispersive components. XPS and SIMS reveals the presence carbon, oxygen and some peaks from substrate including Cr and Fe.

Acknowledgment: Mr. R. Said is grateful to the Libyan government for the Ph.D. financial support.

References and Notes

1. A. Grill, *Thin Solid Films* 355–356, 189 (1999).
2. C. Corbella, G. Oncins, M. A. Gomez, M. C. Polo, E. Pascual, J. Garcia-Cespedes, J. L. Andujar, and E. Bertran, *Diamond Relat. Mater.* 14, 1103 (2005).
3. M. J. Mirtich, D. Nir, D. Swec, and B. Banks, *J. Vac. Sci. Technol. A* 4, 2680 (1986).
4. T. J. Moravec and J. C. Lee, *J. Vac. Sci. Technol.* 20, 338 (1986).
5. M.-S. Hwang and C. Lee, *Mater. Sci. Eng., B* 75, 24 (2000).
6. F. Ma, G. Li, H. Li, H. Ma, and X. Cai, *Mater. Lett.* 57, 82 (2002).
7. H. Li, T. Xu, C. Wang, J. Chen, H. Zhou, and H. Liu, *Diamond Relat. Mater.* 15, 1228 (2006).
8. S. Miyake, T. Saito, Y. Yasuda, Y. Okamoto, and M. Kano, *Tribology International* 37, 751 (2004).
9. J. C. Sanchez-Lopez, C. Donnet, J. Fontaine, M. Belin, A. Grill, V. Patel, and C. Jahnes, *Diamond Relat. Mater.* 9, 638 (2000).
10. B. D. Beake and S. P. Lau, *Diamond Relat. Mater.* 14, 1535 (2005).

11. G. J. Wan, P. Yang, R. K. Y. Fu, Y. F. Mei, T. Qiu, S. C. H. Kwok, J. P. Y. Ho, N. Huang, X. L. Wu, and P. K. Chu, *Diamond Relat. Mater.* 15, 1276 (2006).
12. G. A. Abbas, P. Papakonstantinou, T. I. T. Okpalugo, J. A. Mcaughlin, J. Filik, and E. Harkin-Jones, *Thin Solid Films* 482, 201 (2005).
13. J. S. Chen, S. P. Lau, Z. Sun, G. Y. Chen, Y. J. Li, B. K. Tay, and J. W. Chai, *Thin Solid Films* 398–399, 110 (2001).
14. S. P. Lau, Y. J. Li, B. K. Tay, Z. Sun, G. Y. Chen, J. S. Chen, and X. Z. Ding, *Diamond Relat. Mater.* 10, 1727 (2001).
15. J. S. Chen, S. P. Lau, B. K. Tay, G. Y. Chen, Z. Sun, Y. Y. Tan, and G. Tan, *J. Appl. Phys.* 89, 7814 (2001).
16. Y. W. Li, C. F. Chen, and Y. J. Tseng, *Jpn. J. Appl. Phys.* 40, 777 (2001).
17. T. Young, *Philos. Trans. R. Soc. Lond.* 9, 255 (1805).
18. J. S. Kim, R. H. Friend, and F. Cacialli, *J. Appl. Phys.* 86, 2774 (1999).
19. S. Adhikari, D. C. Ghimire, H. R. Aryal, G. Kalita, and M. Umeno, *Diamond Relat. Mater.* 17, 696 (2008).
20. R. J. Good, *J. Adhes. Sci. Technol.* 2, 1269 (1992).
21. N. Ali, Y. Kousar, T. I. Okpalugo, V. Singh, M. Pease, A. A. Ogwu, J. Gracio, E. Titus, E. I. Meltis, and M. J. Jackson, *Thin Solid Films* 515, 59 (2006).

Received: 10 December 2008. Accepted: 20 January 2009.

Delivered by Publishing Technology to: Chinese University of Hong Kong
IP: 104.169.69.239 On: Wed, 24 Feb 2016 05:59:18
Copyright: American Scientific Publishers